JACS
JOURNAL OF THE AMERICAN CHEMICAL SOCIETY
Article
pubs.acs.org/JACS

Pyrazolate-Based Porphyrinic Metal–Organic Framework with Extraordinary Base-Resistance

Kecheng Wang,[†,‡] Xiu-Liang Lv,[†] Dawei Feng,[‡] Jian Li,[§] Shuangming Chen,[∥] Junliang Sun,[§] Li Song,[∥] Yabo Xie,[†] Jian-Rong Li,[*,†] and Hong-Cai Zhou[*,‡]

[†]Beijing Key Laboratory for Green Catalysis and Separation and Department of Chemistry and Chemical Engineering, College of Environmental and Energy Engineering, Beijing University of Technology, Beijing 100124, P. R. China

[‡]Department of Chemistry, Texas A&M University, College Station, Texas 77842-3012, United States

[§]College of Chemistry and Molecular Engineering, Peking University, Beijing 100871, P. R. China

[∥]National Synchrotron Radiation Laboratory, University of Science and Technology of China, Hefei 230026, P. R. China

Supporting Information

ABSTRACT: Guided by a top-down topological analysis, a metal–organic framework (MOF) constructed by pyrazolate-based porphyrinic ligand, namely, PCN-601, has been rationally designed and synthesized, and it exhibits excellent stability in alkali solutions. It is, to the best of our knowledge, the first identified MOF that can retain its crystallinity and porosity in saturated sodium hydroxide solution (~20 mol/L) at room temperature and 100 °C. This almost pushes base-resistance of porphyrinic MOFs (even if MOFs) to the limit in aqueous media and greatly extends the range of their potential applications. In this work, we also tried to interpret the stability of PCN-601 from both thermodynamic and kinetic perspectives.

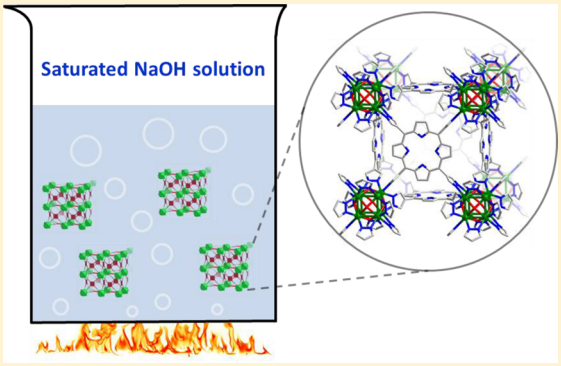

INTRODUCTION

As a novel class of porous materials, metal–organic frameworks (MOFs) have attracted great interest.[1] Their modular nature endows these materials with structural diversity and tunable functionality.[2] One feasible method to functionalize MOFs is to introduce different functional groups via the organic linkers.[3] Porphyrinic derivatives incorporated into MOFs as the organic linkers have been studied tremendously because of their important roles in lots of chemical and biological processes, as well as other applications such as anticancer drugs, catalysts, photosensitizer, pH sensors, etc.[4]

Owing to the fact that many applications of porphyrin involve harsh chemical conditions, chemical stability becomes crucial for porphyrinic MOFs.[5] Therefore, the development of highly stable porphyrinic MOFs is a sought-after goal to extend the scope of applications for these materials. One direct strategy to overcome the vulnerability of MOFs is to enhance the strength of coordination bonds between organic linkers and metal nodes. To realize this, one of the extensively explored methods is to choose secondary building units (SBUs) formed with high-valent metal ions and carboxylate groups, like $[Zr_6O_4(OH)_4(CO_2)_{12}]$ and $[M_3OX(CO_2)_6]$ (M = Al^{3+}, Cr^{3+}, or Fe^{3+}; X = OH^-, F^-, or Cl^-).[6] With this strategy, several porphyrinic MOFs with high stability in acidic and neutral aqueous solutions have been obtained, such as PCN-22X (X = 2, 3, 4, and 5), PCN-600, and Al-PMOF.[5,7]

However, these acid-resistant MOF materials usually are fragile in basic aqueous solutions, which could severely hamper some of their applications.[8] A typical example is PCN-222 (or MOF-545).[3e,5a] It can even survive in concentrated hydrochloride acid, but it decomposes easily in dilute alkali solution.[5a] Since azolate-based MOFs, especially pyrazolate-based ones (pyrazolate is shorten as Pz), have been demonstrated to be extremely stable under basic environments,[9] adopting Pz-based porphyrinic organic linkers thus becomes a promising way to obtain base-resistant porphyrinic MOFs.

Herein, we demonstrate how a rational top-down strategy based on topological analysis guides us to obtain a Pz-based porphyrinic MOF with excellent base-resistance, namely, PCN-601, which is constructed by $[Ni_8(OH)_4(H_2O)_2Pz_{12}]$ (denoted as $[Ni_8]$) nodes and 5,10,15,20-tetra(1*H*-pyrazol-4-yl)-porphyrin (H_4TPP) ligands (Figure 1). Experimental data confirm PCN-601 is immune to the attack of H_2O and OH^- in aqueous solutions, even at high temperature. As far as we know, it is the first identified MOF that can retain crystallinity and porosity in saturated NaOH solution at room temperature (RT) and 100 °C.

Received: October 21, 2015
Published: December 30, 2015

DOI: 10.1021/jacs.5b10881
J. Am. Chem. Soc. 2016, 138, 914–919

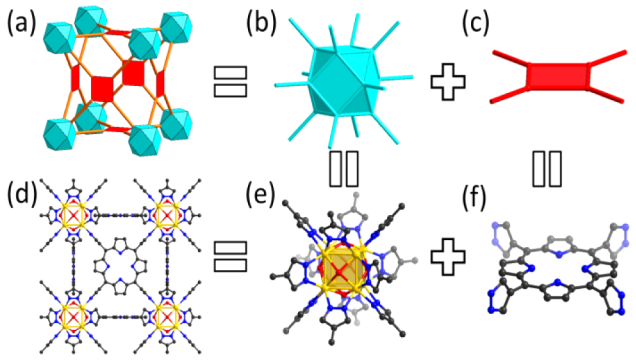

Figure 1. Structural analysis of PCN-601. (a) **ftw-a** topology; (b) O_h symmetric 12-connected node; (c) D_{4h} symmetric 4-connected node; (d) PCN-601 (Ni atoms in the porphyrin center are omitted for clarity); (e) [Ni_8] cluster moiety; (f) TPP^{4-} ligand.

EXPERIMENTAL SECTION

General Information. The commercial chemicals are used as purchased unless mentioned otherwise. Detailed chemical sources are listed in the Supporting Information.

Instrumentation. High-resolution powder X-ray powder diffraction (PXRD) was performed on a PANalytical X'Pert PRO diffractometer equipped with a Pixel detector and using Cu Kα1 radiation (λ = 1.5406 Å). The powder samples were placed in a 0.4 mm diameter glass capillary that was spun during the experiment. Other PXRD was carried out with a BRUKER D8-Focus Bragg–Brentano X-ray powder diffractometer equipped with a Cu sealed tube (λ = 1.54178 Å) at 40 kV and 40 mA. N_2 adsorption–desorption isotherms were measured using a Micrometritics ASAP 2420 system at 77 K. The UV–vis absorption spectra were recorded on a Shimadzu UV-2450 spectrophotometer. X-ray absorption spectroscopy (XAS) measurements were performed in the transmission mode at the beamline 14W1 in Shanghai Synchrotron Radiation Facility (SSRF).

Synthesis of H_4TPP. The synthesis procedure is shown in Scheme 1, and details are in section 2 of the Supporting Information.

Scheme 1. Synthesis of H_4TPP Ligand

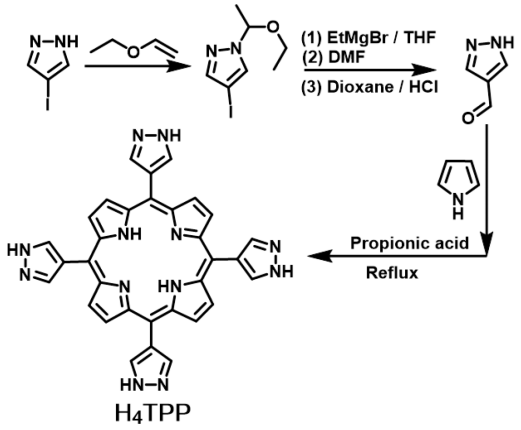

Synthesis of PCN-601. $Ni(AcO)_2{\cdot}4H_2O$ (800 mg), H_4TPP (400 mg), Et_3N (2 mL), and water (8 mL) in 80 mL of *N*,*N*-dimethylformamide (DMF) were ultrasonically dissolved in a 150 mL high-pressure vessel. The mixture was heated at 75 °C for 4 days. After cooling down to room temperature, reddish crystalline powder in colorless solution was obtained. The scanning electron microscope (SEM) image indicates that the crystal size of obtained powder is ~100 nm (Figure S2 in the Supporting Information). Thermogravimetry analysis reveals that the thermal stability of PCN-601 can be held up to 300 °C, at which point it begins to decompose (Figure S3 in the Supporting Information).

Rietveld Refinement and Crystallographic Data of PCN-601. The Rietveld refinement of PCN-601 against PXRD data was performed using Topas v4.2. The background was fitted with a 21st-order Chebychev polynomial. The refinement was conducted using a Thompson–Cox–Hastings pseudo-Voight peak profile function, followed by refinement of unit cells and zero-shift. The rigid bodies were applied on the porphyrin ligand. The unit cell parameters were determined directly from the high solution PXRD pattern by TREOR.[10] Thirty diffraction peaks were used to index (Table S1 in the Supporting Information). The diffraction intensities were extracted by Le Bail fitting using JANA2006. We applied charge-flipping iterations on the extracted intensities using the software Superflip.[11] From the best electron density maps with the lowest R-values, the space group (*Pm*-3*m*) and the position of Ni and O were determined. Other framework atoms were located from the difference Fourier maps; the occupancies were confirmed by inductively coupled plasma (ICP) and elemental analysis (EA) (Figure S5 and Table 1; details are in section 6 of the Supporting Information).

Table 1. Crystallographic Data, Experimental Conditions for PXRD Data Collection, and the Rietveld Refinement Result of PCN-601

chemical formula	$Ni_{9.77}C_{56.64}N_{21.24}O_{10.92}H_{43.75}$
formula weight	1734.20
density (calculated)	0.785
crystal system	cubic
space group	*Pm*-3*m*
a /Å	15.4292(9)
Z	1
temperature/K	298(2)
X-ray source	Cu Kα1
wavelength/Å	1.540596
2θ range/deg	4.502–60.012
number of reflections	146
number of data points	4271
refinement method	Rietveld refinement
Rp	0.0427
Rwp	0.0566
Rexp	0.0321
GOF	1.765
*R*_bragg	0.0130

Gas Adsorption of PCN-601. The reddish powder of PCN-601 obtained through solvothermal reaction was washed with deionized (DI) water several times to remove excess inorganic salt. Then the sample was washed with acetone three times. After being soaked in acetone for an additional 12 h, the sample was activated at 100 °C under vacuum for 12 h. Then, its N_2 uptake was measured at 77 K.

PXRD Measurements for Stability Test of PCN-601. After being washed with DI water, as-obtained PCN-601 samples, 10 mg for each batch, were immersed in about 3.5 mL of aqueous solution of 0.01 mmol/L HCl, 0.1 mmol/L HCl, 0.1 mol/L NaOH, 1 mol/L NaOH, 10 mol/L NaOH, and saturated NaOH (the solution is concentrated with NaOH at 20 °C, which means the concentration is ~109 g of NaOH/100 g of H_2O or 20 mol/L) at room temperature or 100 °C for 24 h. The treated samples were washed with DI water (three times) and acetone (three times). The powders were dried under vacuum at 100 °C for 10 h before PXRD measurements.

N_2 Uptakes for Stability Test of PCN-601. Two batches of samples (~100 mg for each) were immersed in 35 mL of 0.1 mM HCl solution (at room temperature) and saturated NaOH solution (at 100 °C) for 24 h, respectively. After being washed with water (three times) and acetone (three times), the samples were degassed on an ASAP 2420 adsorption system for 10 h at 100 °C. These samples were then measured for N_2 adsorption at 77 K.

DOI: 10.1021/jacs.5b10881
J. Am. Chem. Soc. 2016, 138, 914–919

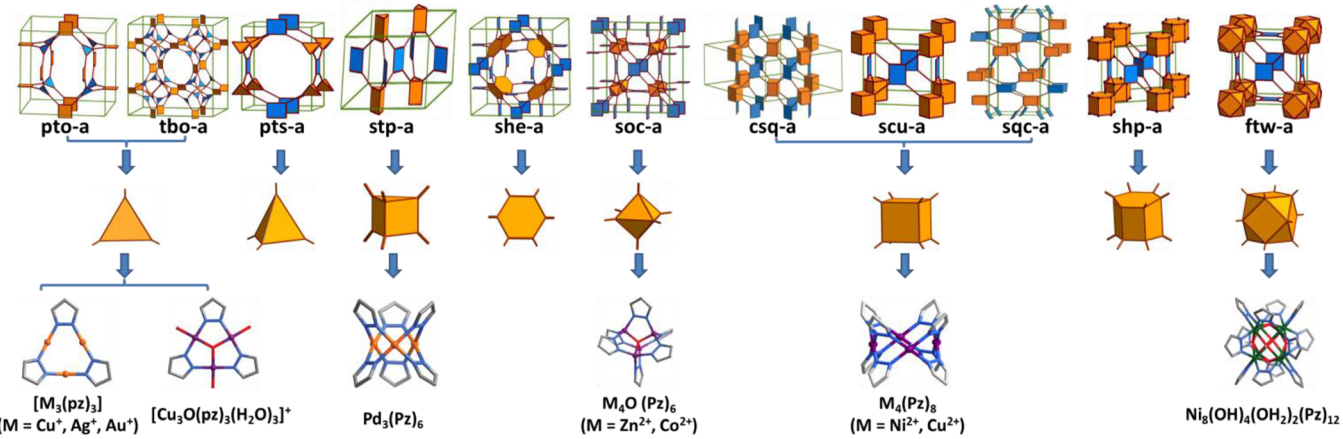

Figure 2. Top-down topological analysis: binodal edge-transitive topologies with planar 4-connected nodes (top line), the nodes assigned to SBUs in corresponding nets (middle line), and reported Pz-based SBUs with the same symmetries and connectivities to corresponding nodes (bottom line).[9b−d,12,13] For the simplification of figure and the absence of reported planar 4-connected Pz-based SBU, the five topologies derivated from uninodal edge-transitive nets with only 4-connected planar nodes are omitted here: **ssb-a**, **ssa-a**, **rhr-b**, **nbo-b**, and **lvt-b**. Some pictures are reproduced with permission from refs 9b and 12. Copyright 2012 American Chemical Society and 2006 International Union of Crystallography, respectively.

UV−Vis Spectra for Stability Test of PCN-601. Two batches of samples (~5 mg for each) were immersed in 3.5 mL of 0.1 mM HCl solution (at room temperature) and saturated NaOH solution (at 100 °C) for 24 h, respectively. After being washed with DI water (three times), the samples were soaked in DMF for 24 h. The clear solutions were taken for UV−vis spectrum measurements. The standard solution of H_4TPP was prepared by dissolving 1 mg of H_4TPP in 20 mL of DMF.

RESULTS AND DISCUSSION

Despite the well-known high robustness of Pz-based MOFs, researchers have faced great difficulty in synthesizing these materials. Unlike with carboxylate-based MOFs, it is much more difficult to obtain single crystals or even highly crystalline powders of Pz-based MOFs, which makes structure determination challenging.[9g,13] To alleviate such challenges and obtain our desired product, a top-down strategy based on topological analysis is applied here. First, we find out the possible topologies and structures that can theoretically incorporate our desired organic linkers. After limiting our preferred products to certain networks, we then rationally choose suitable SBUs and porphyrinic ligands with proper symmetry and geometry, which can fit into targeted structures. Finally, a synthetic condition that can generate our selected SBU is adopted to obtain our expected frameworks. In this way, the time-consuming explorative synthetic work can be minimized and a matched structure can be easily identified by comparison with the proposed framework.

In the first step of the top-down strategy, to make searching of suitable topologies easier, we start from the simplest situation by restricting ourselves to MOFs containing only one kind of SBU, one kind of organic linker, and one kind of connecting edge, which are defined as binodal edge-transitive nets.[9a] Because tetratopic porphyrinic ligands are most frequently adopted in MOFs due to their relative ease of synthesis, we further zoom into binodal edge-transitive nets with a planar 4-connected node. Herein, we enumerated the reported topologies that satisfy our requirements (Figure 2, top line), analyzed the nodes that can be assigned to SBUs in corresponding nets (Figure 2, middle line; the planar 4-connected node is assigned to porphyrinic linker in each topology), and listed the reported Pz-based SBUs with the same symmetries and connectivities to corresponding nodes (Figure 2, bottom line). Through this top-down analysis, eight candidate structures with different topologies (**pto-a**, **tbo-a**, **stp-a**, **soc-a**, **csq-a**, **scu-a**, **sqc-a**, and **ftw-a**) constructed by six kinds of SBUs are generated. Among these SBUs, $[Ni_8(OH)_4(H_2O)_2Pz_{12}]$ (shortened as $[Ni_8]$), a 12-connected cluster with O_h symmetry, is very intriguing to us.[13] This is because it owns the highest connectivity in reported Pz-based SBUs, which empirically can increase the robustness of MOFs.[5c] Thus, a **ftw-a** network constructed by $[Ni_8]$ and Pz-based tetratopic porphyrinic ligand becomes our target.

After determination of the topology and the SBU of our desired MOF, the next step is to consider the geometry details of Pz-based tetratopic porphyrinic ligand. Because the ligand is assigned to the 4-connected node with D_{4h} (or 4/mmm) symmetry in a **ftw-a** topology, only two possibilities are left here: the 4 peripheral Pz groups could be either perpendicular or parallel to the porphyrin center. To determine which type of ligands we should use, we picked PCN-221 as a reference for analysis (Figure 3) because it is also a porphyrinic MOF with **ftw-a** topology.[14] In PCN-221, the SBU is both symmetrically and geometrically equivalent to $[Ni_8]$. Although when the $[Zr_8O_6(CO_2)_{12}]^{8+}$ (denoted as $[Zr_8]$) is simplified into a topological node, it is compatible with two topologically identical tetratopic porphyrinic linkers with D_{4h} symmetry,[5c] in the real MOF construction only one type of linker fits when the spatial arrangement of $[Zr_8]$ and porphyrinic linker is taken into account (Figure S4 in the Supporting Information). Therefore, to construct MOF isostructural to PCN-221, the ligand we use should also be geometrically equivalent to the ligand in PCN-221, which is tetrakis(4-carboxyphenyl) porphyrin (H_4TCPP). As four peripheral benzoates are perpendicular to the porphyrin center in $TCPP^{4-}$ (Figure 3c), we finally choose to construct our targeted MOF with H_4TPP, in which four Pz groups are forced vertical to the porphyrin center because of the steric hindrance of pyrrole rings (Figure 3i).

To obtain our hypothetical structure, the last step here is to explore the synthetic condition to generate the desired cluster. $[Ni_8]$, as isolated cluster, has been synthesized with $Ni(AcO)_2$·

DOI: 10.1021/jacs.5b10881
J. Am. Chem. Soc. 2016, 138, 914−919

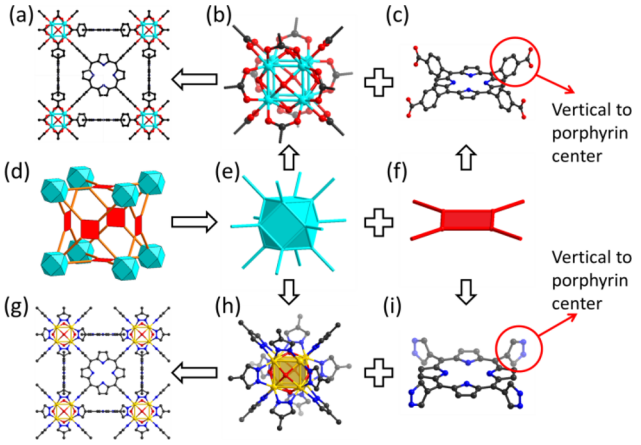

Figure 3. Topological and geometrical analyses of PCN-221 and PCN-601: (a) PCN-221; (b) $[Zr_8O_6(CO_2)_{12}]^{8+}$ cluster moiety; (c) $TCPP^{4-}$; (d) **ftw-a** topology; (e) O_h symmetric 12-connected node; (f) D_{4h} symmetric 4-connected node; (g) PCN-601 (Ni atoms in the porphyrin center are omitted for clarity); (h) $[Ni_8]$ cluster moiety; (i) TPP^{4-} ligand.

$4H_2O$, pyrazole, and a weak base in MeOH.[13c] Ideally, if we can conduct the synthesis under similar conditions, it is quite possible to obtain our designed structure. However, given the low solubility of H_4TPP in MeOH, the solution for the synthesis of our targeted MOF needs to be optimized. Considering the deprotonation of H_2O and Pz groups during the formation of $[Ni_8]$ and the high pK_a values of these two species, we propose that a weak base might be feasible during synthesis of our desired MOF. After dozens of trials, crystalline powder of PCN-601 was finally obtained through the solvothermal reaction of H_4TPP, $Ni(AcO)_2{\cdot}4H_2O$, water, and triethylamine (Et_3N) in DMF.

Guided by the predicted structure, the model of PCN-601 with a space group of *Pm*-3*m* was constructed by Material Studio 6.0.[15] The unit cell parameter of $a = b = c = 15.43$ Å was obtained through indexing experimental high-resolution powder X-ray diffraction (PXRD) data. The predicted structure was ultimately validated with Rietveld refinements (Figure 4). In addition, XAS analysis of PCN-601 sample also suggests that the Ni atom lies in a high symmetrical position such as octahedral center, which is consistent with the refined structure (Figure S6 in the Supporting Information).

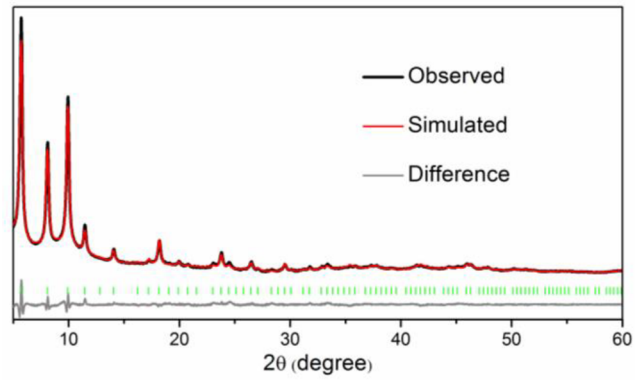

Figure 4. Rietveld refinement of PXRD data for PCN-601. The curves are simulated (red), observed (blue), and difference profiles (gray), respectively; the bars below curves indicate peak positions.

N_2 adsorption/desorption isotherms of PCN-601 at 77 K were performed, after washing and activation of the as-synthesized powder (Figures 5b and S8). A Brunauer–

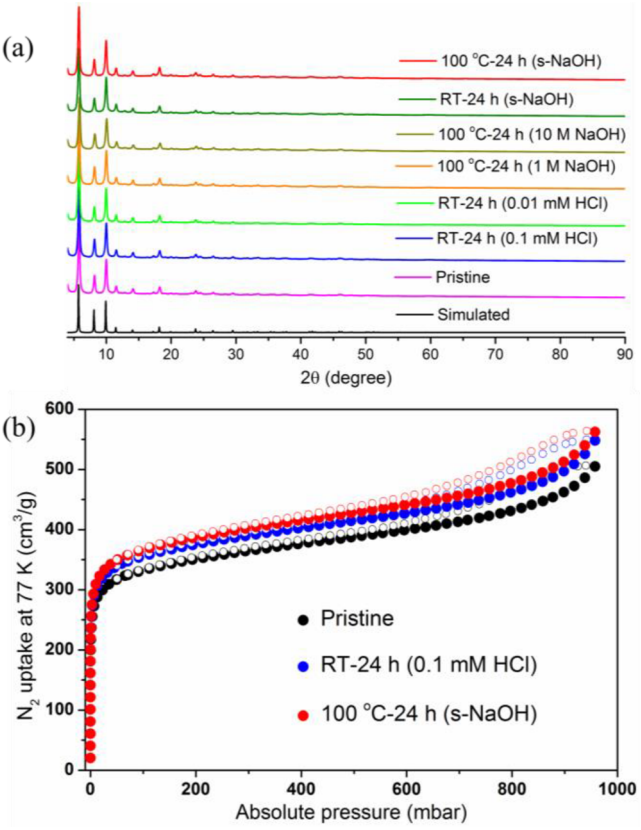

Figure 5. (a) PXRD patterns for simulated, pristine PCN-601, and PCN-601 samples treated under different conditions; (b) N_2 adsorption/desorption isotherms at 77 K of pristine PCN-601 and acid- and base-treated PCN-601 samples.

Emmett–Teller (BET) surface area of 1309 $m^2\ g^{-1}$ and a N_2 uptake of 505 $cm^3\ g^{-1}$ were observed (Figure S9 in the Supporting Information). Evaluation of a density functional theory (DFT) simulation from the N_2 sorption curve suggested the pore size distribution curve reached the maximum around 1.1 nm. The very low distributions of pores with larger diameters are possibly caused by the space between nanoparticles and the existence of defects in crystals (Figure S10 in the Supporting Information).[16]

Chemical stability of PCN-601 was then tested by treating its samples under different conditions. It was found that the PXRD patterns of all treated PCN-601 remain intact, which indicated there was no phase transition or framework collapse during treatments (Figure 5a). Moreover, N_2 adsorption isotherms of PCN-601 treated under the harshest conditions further confirmed its viability in these environments (Figure 5b). Although it is not very obvious, the N_2 uptake of PCN-601 after treatments is slightly higher than that of the untreated sample. We propose that this could be explained by the removal of unknown coordination species trapped inside of the framework in as-synthesized samples during the treatment of acid or base solutions, which causes a slight increase of porosity of PCN-601. Such a situation has also been observed in some other MOFs, like PCN-222, PCN-600, MIL-101, and MIL-53.[5d] Additionally, UV–vis adsorption spectra suggested that the

DOI: 10.1021/jacs.5b10881
J. Am. Chem. Soc. 2016, 138, 914–919

ligand of PCN-601 did not leak into DMF solution even when the samples were treated under the harshest conditions, which also proved the intactness of PCN-601 in stability tests (Figure 6).

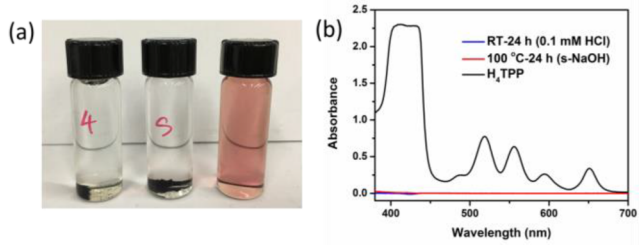

Figure 6. (a) DMF solutions with immersed PCN-601 samples being treated under 0.1 mM HCl solution at room temperature for 24 h (left) and saturated NaOH at 100 °C for 24 h (middle), respectively. In the right vial it is the standard solution of H_4TPP in DMF (1 mg/20 mL). (b) UV–vis spectra of different DMF solutions from the vials in (a).

We propose that the extreme robustness of PCN-601 in basic aqueous media could be explained from both thermodynamic and kinetic perspectives. In basic condition, the decomposition procedure of PCN-601 could be considered as a competition between Pz^- and OH^- (or H_2O) for Ni^{2+}. Compared to OH^- and H_2O, Pz^- has higher crystal field splitting parameter.[17] According to crystal field theory, the coordination between Ni^{2+} and Pz^- can provide more crystal field stabilization energy than that between Ni^{2+} and OH^- (or H_2O). This thermodynamically endows PCN-601 with strong resistance to the attack of H_2O and OH^- even under extremely basic condition (details are in section 10 of the Supporting Information). However, in acidic solution, the major driving force of MOF decomposition becomes the competition between H^+ and Ni^{2+} for Pz^-. Because of the high pK_a value of pyrazole, the equilibrium is more inclined to the decomposed state (Scheme 2a). Therefore, both comparative acid-lability and extreme base-resistance of PCN-601 are related to its different thermodynamic behaviors in acid and base.

From a kinetic aspect, the decomposition of MOFs in solution generally could be considered as a successive substitution reaction, during which defects are generated through replacing coordination moieties of ligands with small molecules or ions, akin to H_2O and OH^-.[18] With respect to the ligand, when one coordination site is displaced from the metal node, it might still stay around because of the restriction from other attached "arms" of ligands. This generates a very high "effective concentration" of coordination moiety around the defect site. Therefore, the rate of reverse reaction for the dissociated site to reattach to the metal nodes is extremely fast,[19] which results in immediate structure reparation. When the connectivity of ligand is higher, this effect will become stronger, because the ligand could tolerate the displacements of more coordination sites and still keep a high rate of defect repair. We call this a "three-dimensional (3D) chelating effect" because of its similarity to the chelating effect in soluble coordination compound. A similar conclusion can be drawn if SBU is considered as the leaving moiety, where high connectivity of SBU will also enhance the stability of the framework. Overall, when the connectivities of the ligand and SBU are high, partial ligand dissociation can hardly result in collapse of the whole framework because of the fast structure reparation. Therefore, such a 3D chelating effect can contribute to the kinetic inertness of MOFs with highly connected SBUs and ligands. Besides the 3D chelating effect, activation energy is another critical factor in decomposition reactions of MOFs. Scheme 2b is a model to compare decomposition processes of two isoreticular MOFs with short and long ligands, noted as MOF-s and MOF-l, respectively. For simplification, we first assume SBUs in these two MOFs are ideally rigid. No matter whether the substitution reactions undergo association or dissociation mechanism, ligands coordinated to SBUs need to be bent in transition states. When the displacements of terminals of ligands in transition states are equal in these two MOFs ($d_s = d_l$), apparently the shorter ligand will be bent more severely ($\theta_s > \theta_l$), which leads to a higher activation energy. As a result, MOFs becomes comparatively inert.[20] On the other hand, both rigidities of SBUs and ligands should also be taken into account in real situations. Reasonably, SBUs and ligands with higher connectivities will be stiffer, which makes MOFs constructed by them more stable.[3c] Given the facts that TPP^{4-} is the shortest porphyrinic ligand in reported porphyrinic MOFs and both $[Ni_8]$ and TPP^{4-} have high connectivities, it is quite natural for PCN-601 to be kinetically stable.

Scheme 2. (a) Thermodynamic Stability of PCN-601 in Acid and Base Conditions; (b) Kinetic Stability of MOFs with Different Lengths of Ligands: d_s and d_l Are the Displacements of Terminals of Ligands in Transition States and θ_s and θ_l Are the Bending Angles of Ligands in Transition States

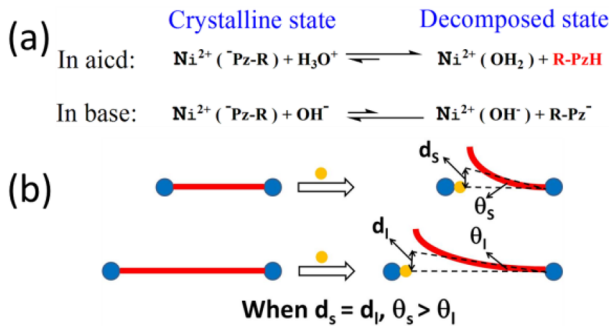

In summary, guided by a top-down topological analysis, we rationally designed and synthesized PCN-601. Its stability has been carefully explored. PXRD and N_2 adsorption suggested its crystallinity and porosity were perfectly maintained in saturated NaOH solution (20 mol/L) at RT and 100 °C. This not only pushes base-resistance of porphyrinic MOFs to the limit in aqueous media but also greatly extends the scope of applications for these materials. We also proposed thermodynamic and kinetic factors that might induce extraordinary robustness of PCN-601 in basic conditions. The extreme robustness in alkali aqueous media indeed endows PCN-601 with unique advantages in many applications, like pH sensing, catalysis, and photodynamic therapy, that may have a high requirement for base-resistance of MOFs.[3e,5b,8] The exploration of PCN-601's performances in these applications is now underway.

■ ASSOCIATED CONTENT

Supporting Information

The Supporting Information is available free of charge on the ACS Publications website at DOI: 10.1021/jacs.5b10881.

DOI: 10.1021/jacs.5b10881
J. Am. Chem. Soc. 2016, 138, 914–919

Full details for the synthesis and characterizations of the MOF, SEM, FT-IR, UV−vis, N_2 isotherms, BET calculation, pore size distribution, XAS analysis, and thermal and chemical stability check (PDF)
Crystallographic data of the refined structure (CIF)

AUTHOR INFORMATION

Corresponding Authors

*jrli@bjut.edu.cn
*zhou@chem.tamu.edu

Author Contributions

K.W. and X.L. contributed equally to this work.

Notes

The authors declare no competing financial interest.

ACKNOWLEDGMENTS

This work was financially supported from the Natural Science Foundation of China (21322601, 21576006, 21271015, and U1407119) and the Program for New Century Excellent Talents in University of China (NCET-13-0647). The synthesis of MOFs and their characterizations were supported as part of the Center for Gas Separations Relevant to Clean Energy Technologies, an Energy Frontier Research Center funded by the U.S. Department of Energy, Office of Science, and Office of Basic Energy Sciences under Award No. DE-SC0001015.

REFERENCES

(1) (a) Zhou, H.-C.; Kitagawa, S. *Chem. Soc. Rev.* **2014**, *43*, 5415. (b) Horcajada, P.; Gref, R.; Baati, T.; Allan, T. P. K.; Maurin, G.; Couvreur, P.; Férey, G.; Morris, R. E.; Serre, C. *Chem. Rev.* **2012**, *112*, 1232. (c) Kreno, L. E.; Leong, K.; Farha, O. K.; Allendorf, M.; Van Duyne, R. P.; Hupp, J. T. *Chem. Rev.* **2012**, *112*, 1105. (d) Suh, M. P.; Park, H. J.; Prasad, T. K.; Lim, D.-W. *Chem. Rev.* **2012**, *112*, 782. (e) Gu, Z.-Y.; Yang, C.-X.; Chang, N.; Yan, X.-P. *Acc. Chem. Res.* **2012**, *45*, 734. (f) Farrusseng, D.; Aguado, S.; Pinel, C. *Angew. Chem., Int. Ed.* **2009**, *48*, 7502.

(2) (a) Sumida, K.; Rogow, D. L.; Mason, J. A.; McDonald, T. M.; Bloch, E. D.; Herm, Z. R.; Bae, T.-H.; Long, J. R. *Chem. Rev.* **2012**, *112*, 724. (b) Yoon, M.; Srirambalaji, R.; Kim, K. *Chem. Rev.* **2012**, *112*, 1196. (c) Cui, Y.; Yue, Y.; Qian, G.; Chen, B. *Chem. Rev.* **2012**, *112*, 1126. (d) Li, J.-R.; Sculley, J.; Zhou, H.-C. *Chem. Rev.* **2012**, *112*, 869. (e) Wu, H.; Gong, Q.; Olson, D. H.; Li, J. *Chem. Rev.* **2012**, *112*, 836. (f) Wang, C.; Zhang, T.; Lin, W. *Chem. Rev.* **2012**, *112*, 1084. (g) Corma, A.; García, H.; Llabres i Xamena, F. X. *Chem. Rev.* **2010**, *110*, 4606. (h) Umemura, A.; Diring, S.; Furukawa, S.; Uehara, H.; Tsuruoka, T.; Kitagawa, S. *J. Am. Chem. Soc.* **2011**, *133*, 15506.

(3) (a) Lin, Q.; Bu, X.; Kong, A.; Mao, C.; Zhao, X.; Bu, F.; Feng, P. *J. Am. Chem. Soc.* **2015**, *137*, 2235. (b) Gao, W.-Y.; Chrzanowski, M.; Ma, S. *Chem. Soc. Rev.* **2014**, *43*, 5841. (c) Wang, X.-S.; Chrzanowski, M.; Wojtas, L.; Chen, Y.-S.; Ma, S. *Chem. - Eur. J.* **2013**, *19*, 3297. (d) Zhang, Z.; Zhang, L.; Wojtas, L.; Eddaoudi, M.; Zaworotko, M. J. *J. Am. Chem. Soc.* **2012**, *134*, 928. (e) Morris, W.; Volosskiy, B.; Demir, S.; Gándara, F.; McGrier, P. L.; Furukawa, H.; Cascio, D.; Stoddart, J. F.; Yaghi, O. M. *Inorg. Chem.* **2012**, *51*, 6443. (f) Son, H.-J.; Jin, S.; Patwardhan, S.; Wezenberg, S. J.; Jeong, N. C.; So, M.; Wilmer, C. E.; Sarjeant, A. A.; Schatz, G. C.; Snurr, R. Q.; Farha, O. K.; Wiederrecht, G. P.; Hupp, J. T. *J. Am. Chem. Soc.* **2013**, *135*, 862.

(4) (a) Park, J.; Feng, D.; Yuan, S.; Zhou, H.-C. *Angew. Chem., Int. Ed.* **2015**, *54*, 430. (b) Lo, P.-C.; Leng, X.; Ng, D. K. P. *Coord. Chem. Rev.* **2007**, *251*, 2334. (c) Wagenknecht, H.-A. *Angew. Chem., Int. Ed.* **2009**, *48*, 2838. (d) Sun, R. W.-Y.; Che, C.-M. *Coord. Chem. Rev.* **2009**, *253*, 1682.

(5) (a) Feng, D.; Gu, Z.-Y.; Li, J.-R.; Jiang, H.-L.; Wei, Z.; Zhou, H.-C. *Angew. Chem., Int. Ed.* **2012**, *51*, 10307. (b) Jiang, H.-L.; Feng, D.; Wang, K.; Gu, Z.-Y.; Wei, Z.; Chen, Y.-P.; Zhou, H.-C. *J. Am. Chem. Soc.* **2013**, *135*, 13934. (c) Liu, T.-F.; Feng, D.; Chen, Y.-P.; Zou, L.; Bosch, M.; Yuan, S.; Wei, Z.; Fordham, S.; Wang, K.; Zhou, H.-C. *J. Am. Chem. Soc.* **2015**, *137*, 413. (d) Wang, K.; Feng, D.; Liu, T.-F.; Su, J.; Yuan, S.; Chen, Y.-P.; Bosch, M.; Zou, X.; Zhou, H.-C. *J. Am. Chem. Soc.* **2014**, *136*, 13983.

(6) (a) Biswas, S.; Ahnfeldt, T.; Stock, N. *Inorg. Chem.* **2011**, *50*, 9518. (b) Carboni, M.; Abney, C. W.; Liu, S.; Lin, W. *Chem. Sci.* **2013**, *4*, 2396. (c) Kim, M.; Cohen, S. M. *CrystEngComm* **2012**, *14*, 4096. (d) Gutov, O. V.; Bury, W.; Gomez-Gualdron, D. A.; Krungleviciute, V.; Fairen-Jimenez, D.; Mondloch, J. E.; Sarjeant, A. A.; Al-Juaid, S. S.; Snurr, R. Q.; Hupp, J. T.; Yildirim, T.; Farha, O. K. *Chem. - Eur. J.* **2014**, *20*, 12389. (e) Fei, H.; Cohen, S. M. *Chem. Commun.* **2014**, *50*, 4810. (f) Cavka, J. H.; Jakobsen, S.; Olsbye, U.; Guillou, N.; Lamberti, C.; Bordiga, S.; Lillerud, K. P. *J. Am. Chem. Soc.* **2008**, *130*, 13850. (g) Férey, G.; Mellot-Draznieks, C.; Serre, C.; Millange, F.; Dutour, J.; Surble, S.; Margiolaki, I. *Science* **2005**, *309*, 2040.

(7) Fateeva, A.; Chater, P. A.; Ireland, C. P.; Tahir, A. A.; Khimyak, Y. Z.; Wiper, P. V.; Darwent, J. R.; Rosseinsky, M. J. *Angew. Chem., Int. Ed.* **2012**, *51*, 7440.

(8) (a) Jiang, Q.; Sheng, W.; Tian, M.; Tang, J.; Guo, C. *Eur. J. Org. Chem.* **2013**, *2013*, 1861. (b) Chan, T. L.; To, C. T.; Liao, B.-S.; Liu, S.-T.; Chan, K. S. *Eur. J. Inorg. Chem.* **2012**, *2012*, 485.

(9) (a) Park, K. S.; Ni, Z.; Cote, A. P.; Choi, J. Y.; Huang, R.; Uribe-Romo, F. J.; Chae, H. K.; O'Keeffe, M.; Yaghi, O. M. *Proc. Natl. Acad. Sci. U. S. A.* **2006**, *103*, 10186. (b) Zhang, J.-P.; Zhang, Y.-B.; Lin, J.-B.; Chen, X.-M. *Chem. Rev.* **2012**, *112*, 1001. (c) McDonald, T. M.; D'Alessandro, D. M.; Krishna, R.; Long, J. R. *Chem. Sci.* **2011**, *2*, 2022. (d) Tonigold, M.; Lu, Y.; Mavrandonakis, A.; Puls, A.; Staudt, R.; Möllmer, J.; Sauer, J.; Volkmer, D. *Chem. - Eur. J.* **2011**, *17*, 8671. (e) Herm, Z. R.; Wiers, B. M.; Mason, J. A.; van Baten, J. M.; Hudson, M. R.; Zajdel, P.; Brown, C. M.; Masciocchi, N.; Krishna, R.; Long, J. R. *Science* **2013**, *340*, 960. (f) Biswas, S.; Grzywa, M.; Nayek, H. P.; Dehnen, S.; Senkovska, I.; Kaskel, S.; Volkmer, D. *Dalton Trans.* **2009**, 6487. (g) Colombo, V.; Galli, S.; Choi, H. J.; Han, G. D.; Maspero, A.; Palmisano, G.; Masciocchi, N.; Long, J. R. *Chem. Sci.* **2011**, *2*, 1311. (h) Gao, W.-Y.; Cai, R.; Meng, L.; Wojtas, L.; Zhou, W.; Yildirim, T.; Shi, X.; Ma, S. *Chem. Commun.* **2013**, *49*, 10516. (i) Xue, D.-X.; Cairns, A. J.; Belmabkhout, Y.; Wojtas, L.; Liu, Y.; Alkordi, M. H.; Eddaoudi, M. *J. Am. Chem. Soc.* **2013**, *135*, 7660.

(10) Werner, P. E.; Eriksson, L.; Westdahl, M. J. *J. Appl. Crystallogr.* **1985**, *18*, 367.

(11) Palatinus, L.; Chapuis, G. *J. Appl. Crystallogr.* **2007**, *40*, 786.

(12) (a) Delgado-Friedrichs, O.; O'Keeffe, M.; Yaghi, O. M. *Acta Crystallogr., Sect. A: Found. Crystallogr.* **2006**, *62*, 350. (b) Delgado-Friedrichs, O.; O'Keeffe, M. *Acta Crystallogr., Sect. A: Found. Crystallogr.* **2007**, *63*, 344.

(13) (a) Masciocchi, N.; Galli, S.; Colombo, V.; Maspero, A.; Palmisano, G.; Seyyedi, B.; Lamberti, C.; Bordiga, S. *J. Am. Chem. Soc.* **2010**, *132*, 7902. (b) Padial, N. M.; Quartapelle Procopio, E.; Montoro, C.; Lopez, E.; Oltra, J. E.; Colombo, V.; Maspero, A.; Masciocchi, N.; Galli, S.; Senkovska, I.; Kaskel, S.; Barea, E.; Navarro, J. A. *Angew. Chem., Int. Ed.* **2013**, *52*, 8290. (c) Xu, J.-Y.; Qiao, X.; Song, H.-B.; Yan, S.-P.; Liao, D.-Z.; Gao, S.; Journaux, Y.; Cano, J. *Chem. Commun.* **2008**, *47*, 6414.

(14) Feng, D.; Jiang, H.-L.; Chen, Y.-P.; Gu, Z.-Y.; Wei, Z.; Zhou, H.-C. *Inorg. Chem.* **2013**, *52*, 12661.

(15) *Accelerys Materials Studio Release Notes*, Release 5.5.1; Accelrys Software, Inc.: San Diego, 2010.

(16) (a) Torad, N. L.; Hu, M.; Kamachi, Y.; Takai, K.; Imura, M.; Naito, M.; Yamauchi, Y. *Chem. Commun.* **2013**, *49*, 2521. (b) Zhu, X.; Gu, J.; Wang, Y.; Li, B.; Li, Y.; Zhao, W.; Shi, J. *Chem. Commun.* **2014**, *50*, 8779.

(17) Reedijk, J. *Recl. Trav. Chim. Pays-Bas* **1969**, *88*, 1451.

(18) Low, J. J.; Benin, A. I.; Jakubczak, P.; Abrahamian, J. F.; Faheem, S. A.; Willis, R. R. *J. Am. Chem. Soc.* **2009**, *131*, 15834.

(19) Clarkson, A. J.; Buckingham, D. A.; Rogers, A. J.; Blackman, A. G.; Clark, C. R. *Inorg. Chem.* **2000**, *39*, 4769.

(20) DeCoste, J. B.; Peterson, G. W.; Jasuja, H.; Glover, T. G.; Huang, Y.-G.; Walton, K. S. *J. Mater. Chem. A* **2013**, *1*, 5642.

DOI: 10.1021/jacs.5b10881
J. Am. Chem. Soc. 2016, 138, 914−919